NATIONAL ADVISORY COMMITTEE FOR AERONAUTICS

TECHNICAL NOTE 2462

INFLUENCE OF REFRACTION ON THE APPLICABILITY OF THE

ZEHNDER-MACH INTERFEROMETER TO STUDIES OF

COOLED BOUNDARY LAYERS

By Martin R. Kinsler

Lewis Flight Propulsion Laboratory
Cleveland, Ohio

NACA

Washington

September 1951

1

1

2184

NATIONAL ADVISORY COMMITTEE FOR AERONAUTICS

TECHNICAL NOTE 2462

INFLUENCE OF REFRACTION ON THE APPLICABILITY OF THE ZEHNDER-MACH

INTERFEROMETER TO STUDIES OF COOLED BOUNDARY LAYERS

By Martin R. Kinsler

SUMMARY

In order to determine the applicability of the Zehnder-Mach inter-
ferometer to two-dimensional cooled-boundary-layer studies, an analyti-
cal investigation was conducted. It was found that for low wall to
free-stream temperature ratios, the effects of light refraction may
cause considerable error in the boundary-layer density profiles cal-
culated from interferogram measurements if these effects are not taken
into account and that it is impossible to observe the boundary layer
very close to the cooled wall.

This report therefore contains a discussion of the magnitude of
the refraction effects that may be expected and acts as a guide in the
design of two-dimensional test sections for the study of cooled boundary
layers by the interferometric method.

Equations are derived and used to compute the trajectories of light
rays through particular boundary layers as well as the approximate cor-
rections that must be applied to the boundary-layer density values to
take into account the effects of refraction. The computations were made
for a range of conditions that is mainly of interest in turbine-blade
cooling studies. Laminar and turbulent boundary layers that have a
free-stream Mach number of 1.0, no pressure gradients in the flow
direction, and wall to free-stream temperature ratios from approxi-
mately 0.33 to 0.9 were considered.

INTRODUCTION

In order to predict the heat-transfer to cooled surfaces in hot-
gas streams, local heat-transfer coefficients must be estimated.
Local heat-transfer coefficients can be obtained from interferograms of
the boundary layer about two-dimensional bodies in a free-convection
flow by determining the temperature gradient at the surface of these
bodies (reference 1). For forced convection of hot gases, the boundary
layers are usually very thin and the temperature gradients through the
boundary layer are very large; light rays passing through the boundary

layer will therefore be refracted considerably. Heat transfer is deter-
mined by the region in the boundary layer that is very close to the
surface. When the boundary layer is cooled, light is refracted toward
the surface so that the part of the boundary layer nearest the surface
cannot be observed. Even though it is expected that temperature gradi-
ents at the wall cannot be obtained in this case, the prediction of
heat-transfer coefficients can be greatly facilitated by a knowledge of
flow conditions, such as, how and when transition to turbulence and
separation occur in the boundary layer.

Corrections for the effects of the refraction that are necessary
to obtain the true density or temperature profile of a two-dimensional
boundary layer from interferograms are discussed in reference 2. In a
talk on the accuracy of gas-flow interferometry given at the March 5,
1948 meeting of the Optical Society of America, F. Joachim Weyl dis-
cussed the effects of light refraction on the design of two-dimensional
supersonic wind tunnels. However, the case in which light rays are
bent into the surface was not discussed in either of these references.
It is desired to determine the flow conditions and test-section design
for which the effects of refraction must be considered and to determine
what can be done to minimize these effects.

The investigation reported herein, which was conducted at the NACA
Lewis laboratory, will aid in the estimation of the order of magnitude
of the refraction effects that can be expected in an interferometric
investigation of two-dimensional boundary layers similar to those
encountered in the flow over cooled turbine blades. Numerical results
are obtained for flow in laminar and turbulent boundary layers on a
flat plate at a free-stream Mach number of 1.0 and at wall to free-
stream temperature ratios from approximately 0.33 to 0.9.

METHOD OF ANALYSIS

The interferometer is best suited to two-dimensional studies;
therefore, the boundary layer existing on a cooled model contained in
a rectangular channel will be considered. It is assumed that the model
spans the distance between two glass walls and has its stagnation point
at some point downstream of the entrance to the channel.

It is also assumed that various conditions of pressure, gas veloc-
ity, and temperature can be attained at any point in the channel. The
boundary layer to be investigated is initially laminar and then transi-
tion to turbulence takes place. According to reference 3, transition
can transport itself laterally across the channel by the mechanism of
transverse contamination. In such a case, the transition region is
V-shaped. The glass-wall boundary layer and the boundary layer on the
model surface intersect at the corners of the channel as shown in

2184

figure 1, which is a schematic diagram describing the path a light ray would take when passing through a boundary layer formed in a "two-dimensional" test section during forced-convection flow over a cooled surface. The free-convection boundary layers on the outside of the channel due to the temperature differences between the glass wall and outside air, the nonuniform temperature distribution in the glass walls due to heat flow to the cooled model, and the inside-wall boundary layers as well as the boundary layer under investigation affect the trajectory of a light ray passing through the channel. In this investigation, it is assumed that the outside free convection has been effectively eliminated and that the density gradients in the glass walls and glass-wall boundary layers are parallel to the ray entering the glass wall. A diagram of a test-section design that is expected to allow the previous assumptions to be approximately satisfied.is presented in figure 2. The cooled body is removed from the glass wall in order to reduce the local thermal variation of the index of refraction in the glass wall and to prevent the intersection of the boundary layers at the corners of the channel. The effect of the gap size between the model and the glass on the apparent thickening of the boundary layer has not been investigated, but it is known that removing the cooled body from the window considerably reduces the thermal distortion of the glass. The evacuated chambers on the sides of the channel allow thin glass to be used in the channel wall when the air flow in the channel is at low pressure and eliminate much of the free convection on the outside of the channel. The evacuated chambers require that glass be inserted in the reference path of the interferometer to compensate for the thick glass on the chambers.

The two effects of refraction that will cause difficulties in evaluating interferograms are: (1) The lower light rays are bent into the surface and therefore will not appear at all on an interferogram; (2) Because a light ray passes through regions of varying density, a fringe shift appearing on an interferometer screen indicates a value of the density integrated on a curved light-ray path through the boundary layer.

The first effect is investigated by obtaining an expression for the trajectories of light rays through various laminar and turbulent boundary layers. This expression is presented in a dimensionless form that avoids numerical calculations involving various Reynolds numbers, free-stream densities, light sources of different wavelengths, and distances back from the stagnation point. The form of the expression is such that numerical representations of boundary-layer temperature profiles may be readily substituted.

All symbols are defined in appendix A; the equation of the trajectory of a ray is given in appendix B as:

$$\xi = - \int_{\eta_1}^{\eta} \frac{r^2}{dr/d\eta} \, d\eta \tag{1}$$

where

$$\eta = K \frac{Re^m}{x} y$$

and

$$\xi = \frac{1}{2} (k\rho_\delta) \, K^2 \, Re^{2m} \left(\frac{L'}{x}\right)^2 \left(\frac{z}{L}\right)^2$$

The height parameter η is essentially the ratio of the distance from the surface y to the boundary-layer thickness δ. In the expression for the parameter η it is assumed that the boundary-layer thickness is proportional to some power of x. This kind of behavior is quite often found in laminar and turbulent boundary layers.

The second effect can be estimated by considering that a light ray entering the channel at position y_1 (see fig. 3) appears to traverse the channel at a height y_a and indicates a density ρ_a on an interferogram. The second effect can therefore be described by the ratios ρ_a/ρ_1 and y_a/y_1. The ray that passes through a point at a height y in the test section, reaches an image point on the interferometer screen. The point at a height y_a, or position A in the object plane, corresponds to this image point. In appendix B it is shown that

$$\frac{y_a}{y_1} = \frac{1}{\eta_1} \left(\eta_2 - \epsilon' \, \xi_2 \, \Theta_2\right) \tag{2}$$

where

$$\Theta = \frac{d\eta}{d\xi} = \frac{(L'/z) \, \theta}{K(k\rho_\delta) \, Re^m \, (L'/x)}$$

The equation used to evaluate interferograms where the refraction effects are small is

$$S\lambda = L \, (n_a - n_o) \tag{3}$$

By substituting

$$n = k\rho + 1 \tag{4}$$

for the index of refraction η in equation (3) an expression for the quantity ρ_a can be found. The value of the fringe shift S at the image point which corresponds to y_a in the object plane is to be substituted in the equation in order to obtain ρ_a. In appendix B, the optical-path length $S\lambda$ is also obtained by an integration procedure that takes into account the refraction of the light ray. When both equations for $S\lambda$ are combined

$$\frac{\rho_a}{\rho_1} = \left(\frac{\rho_a}{\rho_1}\right)_f + \left(\frac{\rho_a}{\rho_1}\right)_{1-2} + \left(\frac{\rho_a}{\rho_1}\right)_\Omega \tag{5}$$

where the terms on the right side of the equation are, respectively, the contributions to ρ_a/ρ_1 due to the boundary layers on the glass walls inside the test section, the refraction of a ray through the boundary layer under investigation, and the contribution due to the optical path from a point at the inside of the exit window to the image plane (reference 2). The three contributions were found to be

$$\left(\frac{\rho_a}{\rho_1}\right)_f = 2\,\frac{r_1}{r_f}\,\frac{\delta_f}{L} \tag{6}$$

$$\left(\frac{\rho_a}{\rho_1}\right)_{1-2} = r_1\frac{\left(1-2\frac{\delta_f}{L}\right)}{2\sqrt{\xi_2}}\left(\int_0^{\xi_2}\frac{d\xi}{r\sqrt{\xi}} + \int_0^{\xi_2}\Theta^2\sqrt{\xi}\,d\xi\right) \tag{7}$$

$$\left(\frac{\rho_a}{\rho_1}\right)_\Omega = -\frac{\xi}{2}\,r_1\,\xi_2\,\Theta_2^{\,2} \tag{8}$$

where r_f is an average value of the temperature ratio in the glass-wall boundary layer.

NUMERICAL CALCULATIONS

It is desired to demonstrate the applicability of the preceding analysis in estimating the magnitude of the refraction effects that are encountered in an interferometric investigation of laminar and turbulent boundary layers similar to those encountered on cooled turbine blades and in designing a test section that will be useful in obtaining heat-transfer information from interferograms of the boundary layer.

The numerical calculations described in this section are for flow over a flat plate at a free-stream Mach number of 1.0. However, it is

possible to use the method presented for flows in which there are pressure gradients present and that have Mach numbers other than 1.0. It is not the purpose of this report to describe the effects of light refraction for all free-stream conditions that may be encountered but rather to show general trends that may be expected.

Temperature Profiles

The theoretical temperature profile over a flat plate for a completely laminar boundary layer, as obtained from reference 4 and from additional information supplied to the NACA by Dr. Crocco, is presented in figure 4(a). The ratio of the absolute static temperature in the boundary layer to the absolute free-stream static temperature is plotted against the usual parameter η. The property values assumed in obtaining the boundary-layer temperature profiles are for air and are assumed to vary as a power function of the temperature. The functions used for the viscosity-temperature and specific heat-temperature relations are $\dfrac{\mu}{\mu_\delta} = \left(\dfrac{T}{T_\delta}\right)^{0.75}$ and $\dfrac{c_p}{c_{p,\delta}} = \left(\dfrac{T}{T_\delta}\right)^{0.19}$, respectively. The Prandtl number is equal to 0.725. For laminar boundary layers, the exponent of the Reynolds number is $m = 0.5$ and $K = 1$ in the expression for η.

In order to obtain a corresponding plot for the turbulent boundary layer, the similarity that exists at $Pr = 1$ between the velocity field and the field of total temperature drop (reference 5) is used to obtain an expression for r in terms of η.

$$\frac{u}{U} = \frac{T' - T_w}{T'_\delta - T_w} \tag{9}$$

By substituting

$$T' = T\left(1 + \frac{\gamma-1}{2} M^2\right) \tag{10}$$

and

$$M = M_\delta \frac{u}{U} \sqrt{\frac{1}{r}} \tag{11}$$

for the total temperature and Mach number in equation (9) it can be shown that

$$r = \frac{\gamma-1}{2} M_\delta^2 \frac{u}{U}\left(1 - \frac{u}{U}\right) + r_w\left(1 - \frac{u}{U}\right) + \frac{u}{U} \tag{12}$$

In the turbulent region of the turbulent boundary layer the velocity
profile is approximated by a power law

$$\frac{u}{U} = \left(\frac{y}{\delta}\right)^{1/N} \qquad\qquad (13)$$

Measured velocity profiles for low subsonic flow show that the value
of N can be taken as seven. In reference 6, it is shown that the
boundary layer thickness is $\delta = \dfrac{0.376}{Re^{1/5}} x$ if the 1/7 power law is used.
Then $\eta = \dfrac{y}{\delta} = K \dfrac{Re^m}{x} y$ where $K = 2.66$, and $m = 0.2$.

In the laminar sublayer, it is assumed that

$$\frac{T - T_W}{T_s - T_W} = \frac{u}{U} = \frac{y}{y_s} \qquad\qquad (14)$$

and in reference 6

$$\frac{y_s}{\delta} = \frac{191}{Re^{0.7}} \qquad\qquad (15)$$

for a turbulent boundary layer following the 1/7 power law. From
equations (12), (14), and (15), it can be shown that

$$r = \text{constant } \eta + r_W \qquad\qquad (16)$$

in the laminar sublayer. The temperature ratio for the laminar sub-
layer and the turbulent region are plotted in figure 4(b) for a Mach
number of 1.0. For the laminar sublayer the Reynolds number was chosen
at 5×10^5 in order to obtain the constant in equation (16). The turbu-
lent portion of the profiles described by equation (12) is independent
of Reynolds number as long as the 1/7 power law is valid.

Light-Ray Trajectories

The possibility of calculating trajectories of light rays through
the boundary layer is offered by equation (1). In figure 5, the light
paths through the three laminar and the three turbulent boundary layers
shown in figures 4 and 5 are described. The right side of equation (1)
was evaluated by means of Simpson's rule. The slope of the curves in
figures 6 and 7 depend only upon the parameters η and r_W as shown
in equation (1). Therefore, for any value of η all curves for the
same parameter r_W have the same slope. This fact is helpful
in interpolating values between the curves.

2184

Determination of y_a/y_1

From equation (2), y_a/y_1 is plotted against ξ_2 for various values of r_w and η_1 in figure 6. It is assumed that the object plane corresponds to the center plane of the channel, that is, $\epsilon' = 1 = \xi$.

Determination of ρ_a/ρ_1

An estimate of the quantity ρ_a/ρ_1 for the prescribed boundary layers may be made from figures 7 to 9. In figure 7, $(\rho_a/\rho_1)_f$ is plotted against δ_f/L for various values of the quotient r_1/r_f. Plots of $(\rho_a/\rho_1)_{1-2}$ against ξ_2 for various wall-to-stream temperature ratios and values of η_1 are presented in figure 8. The calculations for these plots were made by assuming, in equation (7), that the glass-wall boundary layer is negligible, that is, $\delta_f/L = 0$. For values of $\delta_f/L > 0$ the ratio, $(\rho_a/\rho_1)_{1-2}$ should be multiplied by $\left(1-2\dfrac{\delta_f}{L}\right)$. The values of $(\rho_a/\rho_1)_{1-2}$, are limited because the rays are bent into the surface.

In figure 9, $(\rho_a/\rho_1)_\Omega$ is plotted against ξ_2 for various temperature ratios and values of η_1. The object plane was assumed to correspond to the plane containing the center plane of the test section.

A Numerical Example

It is desired to design a channel that can be used to obtain local heat-transfer coefficients over a flat surface by means of the Zehnder-Mach interferometer for a given air temperature, wall-to-stream temperature ratio, Reynolds number, and Mach number of the order of magnitude of 1.0. The design procedure consists of assuming various values of the pressure and temperature of the air in the test section and then determining if reasonable values of the fringe shift across the boundary layer, the ratio $\dfrac{x}{L}$, and the ratio $\dfrac{(\rho_a/\rho_1)_f}{\rho_a/\rho_1}$ are obtained. The effects of refraction that can be expected for a particular design must be estimated before these calculations may be made.

In order to obtain the local heat-transfer coefficient directly from the fringe shifts on an interferogram, it is necessary to calculate

the boundary-layer temperature gradient at the wall. However, all light rays are bent toward the surface and it will not be possible to view the boundary layer near the wall. For this reason, it is assumed sufficient to obtain the temperature profile up to the point at which the temperature gradient is 0.9 of the gradient at the wall in the laminar boundary layer and up to a value of $y/\delta = 0.01$ in the turbulent boundary layer. The profile shapes shown in figure 4 were used to determine the corresponding value of η in the present evaluation. In addition, it has been found that it is very difficult to obtain the temperature profile for points that are very close to the wall. The boundary-layer thickness is therefore made large enough so that the portion of the boundary layer which vanishes is at least 0.004 inch.

Because it is desired to keep the glass-wall boundary layer thin it would be helpful to so design the rectangular channel that the length of the wall containing the glass is as short as possible. This design is accomplished by using one wall of the channel as the test surface, which is considered to be cooled over its entire length.

Air at 70° F is assumed to flow through the channel at a maximum Reynolds number of 5×10^5. The pressure in the channel is maintained constant at about 26 inches of mercury vacuum. A test-section design is obtained for three wall-to-stream temperature ratios for both laminar and turbulent boundary layers. The light source in the interferometer is a filtered mercury arc lamp giving off only the green line which has a wave length of 5461 angstrom units.

The results of the calculations are presented in table I. In column 1 of this table, boundary layers having three different wall-to-stream temperature ratios each are selected. In column 2, the minimum values for the distance back from the stagnation point are obtained by substituting the lowest value of η_1 that is desired into the relation $\eta = K \dfrac{Re^m}{x}\, y$ where y is set equal to 0.004 inch and the Reynolds number is the maximum value, 5×10^5. The maximum values for the span, column 3, are obtained from: the value of ξ_2 from figures 5(a) and 5(b), which are plots of the trajectories of light rays through the boundary layer; the maximum Reynolds number; a value of $k\rho_\delta$ corresponding to the green line from a mercury arc lamp; a pressure of 26 inches of mercury vacuum; an air temperature of 70° F; and the value x, in column 1. The ratio z/L' is equal to 1.0 and the maximum velocity, in column 4, is obtained at the maximum Reynolds number. In column 5, values of ϵ at $y_a/y_1 = 1$ are presented; ϵ' is related to ϵ by the relation

$$\epsilon' = \frac{\epsilon L/2 - \delta_f}{L/2 - \delta_f}$$

where δ_f is the glass-wall boundary-layer thickness found by assuming the wall boundary layer to be nearly isothermal and to have its stagnation point at the same point as that for the cooled boundary layer. The values of ρ_a/ρ_1 are found from equations (5) to (8) where r_f is assumed equal to 1 because the glass-wall boundary layers are nearly isothermal and r_1 is the value of r corresponding to η_1. Column 6 gives the differences between the density at position one and the apparent density as compared with the density at position one. In column 7, the fringe shift that will appear on an interferogram between the free stream and the wall is given. The equation for the fringe shift from the free stream to any point in the boundary layer is derived from equations (3) and (4) and is

$$S_{a-\delta} = \frac{L}{\lambda} (k\rho_\delta) \left(\frac{\rho_a/\rho_1}{r_1} - 1 \right) \tag{17}$$

This equation is plotted in figure 10 for the conditions of this problem and for a span of 1 inch. A positive sign for the fringe shift indicates that ρ_a is greater than ρ_δ. This fact is discussed in the next section of this report. The ratios of the minimum distance x to the maximum span is given in column 8. In column 9, the ratios of the portions of ρ_a/ρ_1 that result from the glass-wall boundary layers to the total ρ_a/ρ_1 are listed.

DISCUSSION OF RESULTS

The principal factor, other than the flow conditions, governing a test section design is the estimate of how close to the wall the boundary layer need be studied; that is, a minimum value of y/δ must be chosen. In some cooling studies, it may only be necessary to determine whether a particular portion of a boundary layer is laminar or turbulent or where separation has taken place. These types of investigation should be comparatively simple with the interferometer. For some investigations, however, it is necessary to obtain the temperature gradient at the wall. Because the temperature ratio is less than 1.0 and all rays are bent toward the surface, there is a definite limit as to how close to the surface the boundary layer may be investigated. The restriction on the minimum value of y/δ, for which it is desired to obtain the temperature in the boundary layer, also restricts the boundary-layer thickness δ to some minimum value because there is a minimum value of y for which the profile can be investigated.

In general, there are four effects which limit the minimum y value.

2184

(1) If at best, it is possible to estimate to 1/10 of a fringe in determining the fringe shift, the number of fringe shifts across the boundary layer limits the minimum y value that can be investigated.

(2) Even with no flow over a surface a slight fringe shift is often obtained close to the surface. This shift may be due to reflection of light from the surface. It is conceivable that this reflection limits the accuracy with which fringe shifts can be estimated close to a surface as a result of interference between the survey rays and the reflected rays.

(3) The effect of diffraction of light from the edge of the model results in diffraction fringes parallel to the model surface which cause difficulty in determining the interference fringe shift.

(4) There is also some difficulty in obtaining the exact location of the model surface on an interferogram due to the previously mentioned diffraction effect; the intersection of fringes with the surface therefore cause some error in the measured positions. All these effects contribute to the great difficulty encountered in obtaining the temperature profile in the boundary layer very near to a model surface.

The ratio of the distance from the stagnation point x to the span of a channel L is an indication of the feasibility of a certain test-section design. For large values of the ratio x/L, it can be expected that end effects such as the glass-wall boundary layer and transverse contamination, in the case of laminar boundary layers, will be larger and, accordingly, will influence the interferogram fringe shift to a considerable extent. It is difficult to evaluate the average density in these end-effect regions, therefore it is reasonable to believe that it would be difficult to evaluate interferograms for large values of x/L. This observation is illustrated in columns 8 and 9 of table I. The contribution to ρ_a/ρ_1 due to the glass-wall boundary layers increases as the ratio x/L increases.

The value of ϵ, for $y_a/y_1 = 1$, varies but little from 0.8 for the range of conditions investigated (table I, column 5).

An evaluation procedure based on the assumption that the refraction is small would cause considerable error in the profiles calculated from fringe shifts as evidenced by column 6 of table I. The negative fringe shift in column 7 indicates that it would be possible to obtain a wall temperature greater than the free-stream temperature if a correction were not made for refraction. This result may be in error because terms of higher degree than the second in θ were neglected. The results shown in column 7, however, still show that the effects of refraction increase with decreasing temperature ratio.

For given values of $\xi_2 = \frac{1}{2} K^2 (k\rho_\delta) Re^{2m}\left(\frac{L'}{x}\right)^2$, Reynolds number, and gas temperature; the value of x/L can decrease for decreasing pressure. Furthermore, for a constant Reynolds number and gas temperature, a very low pressure is associated with a high velocity. These conditions of low pressure, high velocity, and small x/L are encountered in hypersonic air-flow channels. However, with the very low pressures encountered in high Mach number flow it can be expected that small fringe shifts will occur across the boundary layer.

The results of a preliminary investigation for the hypersonic range indicate that the interferometric method will not be useful as a means of investigating laminar boundary layers for temperaure ratios near one because of the very small fringe shift across the boundary layer but will be useful for laminar layers with low wall-to-stream temperature ratios. In the case of turbulent boundary layers, investigations in the range of temperature ratios near one are also ruled out because of insufficient fringe shift across the boundary layer and the low wall-to-stream temperature ratio is ruled out because the effects of refraction are expected to make an accurate evaluation of the interferogram impossible.

CONCLUSIONS AND RECOMMENDATIONS

A method has been presented for estimating the effects of light refraction in an interferometric investigation of two-dimensional boundary layers.

From plots of the trajectories of light rays through both laminar and turbulent boundary layers, from calculations of the error involved in not taking into account refraction, and from the results of a numerical example; it was found that the effects of refraction become more pronounced as the wall-to-stream temperature ratio is decreased.

The interferometric method is believed to be limited as a method of obtaining local heat-transfer coefficients for forced-convection flow at low wall-to-stream temperature ratios. The principal cause of the limitation on the method is the large temperature gradient which causes rays to be bent into the surface of the model and prevents the observation of that portion of the boundary layer very close to the wall. In addition, surface reflection, diffraction, and uncertainty in locating the model surface on an interferogram limits measurements on interferograms very near the wall.

It is believed that the interferometer would be useful for investigating laminar boundary layers in hypersonic channels with low wall-to-stream temperature ratios as well as low velocity flows with wall-to-stream temperature ratios near one.

Removal of the cooled model from the glass wall would reduce or eliminate the apparent thickening on interferograms owing to the intersection of the model boundary layer and the glass-wall boundary layers at the concave corners of a channel and reduce or eliminate the thermal distortion of the glass walls that would exist if the model contacted the glass.

The glass wall should be made as thin as possible so that the refraction effects due to any thermal distortion of the glass may be neglected.

In order to allow thin glass windows to be used with a low pressure in the channel it would probably be necessary to provide evacuated chambers on the outside of the channel. The evacuated chambers would have the additional advantage of reducing free convection on the glass test-section walls.

Lewis Flight Propulsion Laboratory,
    National Advisory Committee for Aeronautics,
        Cleveland, Ohio, May 17, 1951.

APPENDIX A

SYMBOLS

The following symbols are used in this report:

c_p specific heat at constant pressure, Btu/(lb)(°F)

c_v specific heat at constant volume, Btu/(lb)(°F)

h $\epsilon \dfrac{L}{2} - \dfrac{T}{3}$, ft

K   constant in the expression $\eta = K \dfrac{Re^m}{x} y$, dimensionless

k   Dale-Gladstone constant, cu ft/slug

L   span, inside test section, ft

L' $L - 2\delta_p$, ft

M   Mach number, dimensionless

m   exponent in the expression $\eta = K \dfrac{Re^m}{x} y$, dimensionless

N   exponent in the expression $(y/\delta)^{1/N}$, dimensionless

n   index of refraction, dimensionless

Pr   Prandtl number, dimensionless

p   static pressure, slugs/sq ft

R   universal gas constant, ft/°R

Re   local Reynolds number $\dfrac{U\rho_\delta x}{\mu_\delta}$, dimensionless

r   temperature ratio $\dfrac{T}{T_\delta}$, dimensionless

S   interferogram fringe shift, dimensionless

s   distance along light path, ft

T   gas static temperature at point x, y, z in the boundary layer, $^\circ$R

T'   gas total temperature, $^\circ$R

U   velocity of gas at outer edge of the boundary layer, ft/sec

u   velocity of gas in x direction, ft/sec

v   velocity of light at point x, y, z; ft/sec

x   distance along surface measured from starting point of boundary
        layer, ft

y   distance normal to the surface, ft

z   distance along span of test section, ft

β   exponent in the specific heat-temperature relation $c_p/c_{p,\delta} = (T/T_\delta)^\beta$

μ   absolute viscosity, slugs/(sec)(ft)

ξ $\frac{1}{2}(k\rho_\delta) K^2 Re^{2m} \left(\frac{L'}{x}\right)^2 \left(\frac{z}{L'}\right)^2$, dimensionless

ρ   density, slugs/cu ft

τ   thickness of glass wall, ft

τ' $\frac{\tau}{\cos(\theta_2/n_g)}$, ft

ω   exponent in viscosity - temperature relation, $\mu/\mu_\delta = (T/T_\delta)^\omega$,
        dimensionless

Subscripts:

a   apparent value

f   inside glass-wall boundary-layer film

g   glass side wall

l laminar boundary layer

o   compensating chamber conditions

s   condition at border of laminar sublayer and turbulent region

t   turbulent boundary layer

γ ratio of specific heats, $\dfrac{c_p}{c_v}$, dimensionless

δ thickness of thermal boundary layer, ft

ϵ ratio of distance between glass and object plane to distance between the glass and test section centerline, dimensionless

ϵ' ratio of distance between position two, figure 3, and object plane to distance between position two and test section centerline, $\dfrac{\epsilon L/2 - \delta_f}{L/2 - \delta_f}$, dimensionless

ζ $\dfrac{z}{L'}$, dimensionless

η $K \dfrac{Re^m}{x} y$, dimensionless

Θ $\dfrac{(L'/z) \theta}{K (k\rho_\delta) Re^m (L'/x)}$, $\dfrac{d\eta}{d\zeta}$, dimensionless

θ slope of ray path at point y, z; dimensionless

λ wavelength of light used, ft

v vacuum

w wall

δ condition at border of boundary layer and free stream

Ω referring to optical path from inside of exit window to the image plane

1   position at which light ray enters boundary layer under investigation

2   position at which light ray leaves the boundary layer under investigation

APPENDIX B

DERIVATION OF EQUATIONS (1) THROUGH (8)

The equation

$$\frac{y''}{1 + y'^2} = -\frac{1}{v}\frac{\partial v}{\partial y} + \frac{1}{v}\frac{\partial v}{\partial z} y' \tag{B1}$$

describes the trajectory of a light ray in a nonhomogeneous medium
(reference 7). By the following substitutions, equation (B1) can be put
in a more useful form:

$$\left.\begin{array}{c} v = \dfrac{v_v}{n} \\[2ex] \dfrac{\partial n}{\partial z} = 0 \\[2ex] y' = \tan\theta \approx \theta \\[2ex] n = k\rho + 1 \\[2ex] k\rho \ll 1 \end{array}\right\} \tag{B2}$$

(for air)

then

$$\frac{d\theta}{dz} = k\frac{d\rho}{dy} \tag{B3}$$

When this equation is integrated with the boundary condition $z = 0$
when $\theta = 0$ yields

$$\theta = k\frac{d\rho}{dy} z \tag{B4}$$

If the equations

$$r = \frac{T}{T_\delta}$$

$$\rho = \frac{p}{RT}$$

$$\eta = K \frac{Re^m}{x} y$$ (B5)

$$\zeta = \frac{z}{L'}$$

are substituted into equation (B4),

$$\frac{d\eta}{d\zeta} = - K^2 (k\rho_\delta) Re^{2m} \left(\frac{L'}{x}\right)^2 \zeta \frac{1}{r^2} \frac{dr}{d\eta}$$ (B6)

By integrating equation (B6) between the limits $\eta = \eta_1$ when $\zeta = 0$ and $\eta = \eta$ when $\zeta = \zeta$ and by substituting

$$2\zeta_2 = K^2 (k\rho_\delta) Re^{2m} \left(\frac{L'}{x}\right)^2$$ (B7)

and

$$\xi = \xi_2 \zeta^2$$ (B8)

then

$$\xi = - \int_{\eta_1}^{\eta} \frac{r^2}{dr/d\eta} d\eta$$ (1)

This equation represents the light-ray trajectories in terms of the new variables.

By letting $\Theta = \frac{d\eta}{d\xi}$, it is found that

$$\theta = \frac{K (k\rho_\delta) Re^m (L'/x)}{\left(\frac{L'}{z}\right)} \Theta$$ (B9)

If the object plane is considered to be at a distance $\epsilon' \dfrac{L'}{2}$ from position 2 in the test section

$$\frac{y_a}{y_1} = \frac{y_2 - \epsilon' \dfrac{L'}{2} \theta_2}{y_1} \tag{B10}$$

where θ is a negative angle.

Substitution of the new variables yields

$$\epsilon' \frac{L'}{2} \frac{\theta_2}{y_1} = \epsilon' \frac{1}{2} (k\rho_\delta) K^2 Re^{2m} \left(\frac{L'}{x}\right)^2 \frac{\Theta_2}{\eta_1} = \xi_2 \frac{\Theta_2}{\eta_1} \epsilon' \tag{B11}$$

and

$$\frac{y_a}{y_1} = \frac{1}{\eta_1} \left(\eta_2 - \epsilon' \xi_2 \Theta_2\right) \tag{2}$$

The relation generally used between index of refraction change and fringe shift (reference 1) is

$$S\lambda = L(n_a - n_o) \tag{3}$$

The optical-path difference between a light path through the test section and a corresponding light path through the compensating section (reference 4) is

$$S\lambda = 2n_f \delta_f + \int_1^2 n \, ds + n_g T' + n_o (h + T) - 2n_o \delta_f -$$

$$n_o L' - n_g T - n_o \left(\frac{h + T}{\cos \theta_2}\right) \tag{B12}$$

By combining equations (3) and (B12), by substituting for the index of refraction

$$n = k\rho + 1 \tag{4}$$

and by solving for $Lk\rho_a$ it is found that

$$Lk\rho_a = 2k\rho_f \ \delta_f + k \int_1^2 \rho \ ds + \frac{1}{2} \int_1^2 \theta^2 \ dz +$$

$$n_g\Delta + \int_1^2 dz - L \tag{B13}$$

where

$$\Delta = \tau' - \tau + \frac{n_o}{n_g}\left(h + \tau\right) - \frac{n_o}{n_g}\left(\frac{h + \tau}{\cos \theta_2}\right) \tag{B14}$$

and where

$$\int ds = \int (1 + \theta^2) \ dz \approx \int \left(1 + \frac{1}{2} \theta^2\right) dz \tag{B15}$$

when powers of θ equal to four or greater are neglected.

If equation (B13) is solved for ρ_a/ρ_1 it can be shown that

$$\frac{\rho_a}{\rho_1} = 2 \ \frac{\rho_f}{\rho_1} \ \frac{\delta_f}{L} + \frac{1}{L} \ \frac{1}{\rho_1} \int \rho \ ds + \frac{1}{2} \ \frac{1}{kL} \ \frac{1}{\rho_1} \int \theta^2 \ dz + \frac{n_g}{k\rho_1} \ \frac{\Delta}{L} \tag{B16}$$

When the temperature ratio $r = T/T_\delta$ and the law of state $\rho = p/RrT_\delta$ are introduced, it follows that

$$\frac{\rho_a}{\rho_1} = 2 \ \frac{r_1}{r_f} \ \frac{\delta_f}{L} + \frac{1}{L} \ r_1 \int \frac{dz}{r} + \frac{1}{2L} \ r_1 \int \frac{\theta^2 \ dz}{r} +$$

$$\frac{1}{2L} \ \frac{1}{k\rho_\delta} \ r_1 \int \theta^2 \ dz + \frac{n_g}{k\rho_\delta} \ r_1 \ \frac{\Delta}{L} \tag{B17}$$

The expression for n_g can be put in the following useful form:

$$n_g\Delta = n_g\tau\left(\frac{1}{\cos\frac{\theta_2}{n_g}} - 1\right) + n_o\tau\left(1 - \frac{1}{\cos\theta_2}\right) + n_o h\left(1 - \frac{1}{\cos\theta_2}\right) \quad \text{(B18)}$$

$$\left(\frac{1}{\cos\frac{\theta_2}{n_g}} - 1\right) \approx \left(\frac{1}{\sqrt{1 - \frac{\theta_2^2}{n_g^2}}} - 1\right) \approx \frac{1}{2}\frac{\theta_2^2}{n_g^2} \quad \text{(B19)}$$

and

$$\left(1 - \frac{1}{\cos\theta_2}\right) \approx -\frac{1}{2}\theta_2^2 \quad \text{(B20)}$$

and because $n_g = 1.5$

$$h = \epsilon\frac{L}{2} - \frac{\tau}{3} \quad \text{(B21)}$$

it can be shown that

$$n_g\Delta = \frac{1}{2}\tau\frac{\theta_2^2}{n_g}\left(1 - n_o n_g - \frac{\epsilon}{2}n_o n_g\frac{L}{\tau} + \frac{1}{3}n_o n_g\right) \quad \text{(B22)}$$

Substituting $n_o = 1$ and $n_g = 3/2$ it is found that

$$\frac{n_g}{k\rho_\delta}r_1\frac{\Delta}{L} = -\frac{\epsilon}{4}r_1\frac{1}{k\rho_\delta}\theta_2^2 \quad \text{(B23)}$$

because

$$\frac{1}{k\rho_\delta} \gg \frac{1}{r}$$

$$\frac{\rho_a}{\rho_1} = 2\frac{r_1}{r_f}\frac{\delta_f}{L} + \frac{r_1}{L}\left(\int_1^2\frac{dz}{r} + \frac{1}{2}\frac{1}{k\rho_\delta}\int_1^2\theta^2\,dz - \frac{\epsilon}{4}\frac{r_1}{k\rho_\delta}\theta_2^2\right)$$
$$\text{(B24)}$$

By substituting the new variables into equation (B24), it can be shown that

$$\frac{\rho_a}{\rho_1} = 2 \, \frac{r_1}{r_f} \, \frac{\delta_f}{L} + r_1 \, \frac{\left(1 - 2\frac{\delta_f}{L}\right)}{2\sqrt{\xi_2}} \left(\int_0^{\xi_2} \frac{d\xi}{r\sqrt{\xi}} + \int_0^{\xi_2} \sqrt{\xi} \, \Theta^2 \, d\xi\right) - \frac{\epsilon}{2} \, r_1 \, \xi_2 \, \Theta_2{}^2$$

(B25)

or

$$\frac{\rho_a}{\rho_1} = \left(\frac{\rho_a}{\rho_1}\right)_f + \left(\frac{\rho_a}{\rho_1}\right)_{1-2} + \left(\frac{\rho_a}{\rho_1}\right)_\Omega$$

(5)

where

$$\left(\frac{\rho_a}{\rho_1}\right)_f = 2 \, \frac{r_1}{r_f} \, \frac{\delta_f}{L}$$

(6)

$$\left(\frac{\rho_a}{\rho_1}\right)_{1-2} = r_1 \, \frac{\left(1 - 2\frac{\delta_f}{L}\right)}{2\sqrt{\xi_2}} \left(\int_0^{\xi_2} \frac{d\xi}{r\sqrt{\xi}} + \int_0^{\xi_2} \Theta^2 \sqrt{\xi} \, d\xi\right)$$

(7)

$$\left(\frac{\rho_a}{\rho_1}\right) = - \frac{\epsilon}{2} \, r_1 \, \xi_2 \, \Theta_2{}^2$$

(8)

REFERENCES

1. Eckert, E. R. G., and Soehngen, E. E.: Studies on Heat Transfer in
   Laminar Free Convection with the Zehnder-Mach Interferometer.
   Tech. Rep. No. 5747, A.T.I. No. 44580, Air Materiel Command,
   Dec. 27, 1948.

2. Ladenburg, R.: Further Interferometric Studies of Boundary Layers
   Along a Flat Plate. Contract No. 47, ONR 399, Task Order I,
   Palmer Physical Laboratory, Dec. 15, 1949.

2184

3. Charters, Alex C., Jr.: Transition between Laminar and Turbulent Flow by Transverse Contamination. NACA TN 891, 1943.

4. Crocco, Luigi: The Laminar Boundary Layer in Gases. Trans. No. F-TS-5053-RE, A.T.I. No. 28323, CADO, Air Materiel Command.

5. Kalikhman, L. E.: Heat Transmission in the Boundary Layer. NACA TM 1229, 1949.

6. Eckert, E. R. G.: Introduction to the Transfer of Heat and Mass. McGraw-Hill Book Co., Inc., 1950, pp. 73-76.

7. Burington, Richard Stevens, and Torrance, Charles Chapman: Higher Mathematics. McGraw-Hill Book Co., Inc., New York, 1939, p. 790.

2184

TABLE I - RESULTS OF NUMERICAL EXAMPLE

[Assumptions: η_1 determined at $dr/d\eta = 0.9(dr/d\eta)_w$ for laminar boundary layer; $\eta_1 = 0.01$ for turbulent boundary layer; minimum $y_1 = 0.004$ in.; maximum $Re = 5 \times 10^5$; pressure = 26 in. Hg vacuum; temperature = 70° F; length of cooled wall = channel length; $k = 0.1166$ ft/slug; $r_f = 1.$]

	1	2	3	4	5	6	7	8	9
	r_w	Minimum x (ft)	Maximum L (in.)	Maximum velocity U (ft/sec)	ϵ at $\dfrac{y_a}{y_1} = 1$	$\dfrac{\rho_1 - \rho_a}{\rho_1}$	$S_{w-\delta}$	x/L	$\dfrac{(\rho_a/\rho_1)_f}{\rho_a/\rho_1}$
Laminar boundary layer	0.343	3.0	1.7	210	0.78	0.12	3.3	21.9	0.13
	.628	1.2	3.1	540	.79	0	2.5	4.5	.04
	.890	1.0	6.8	630	..86	0	1.2	1.8	.02
Turbulent boundary layer	0.333	1.2	1.1	530	0.81	1.12	-2.2	12.8	-3.10
	.5	1.2	1.6	530	.78	.29	.1	9.3	.47
	.8	1.2	2.9	530	.86	.03	.5	4.9	.24
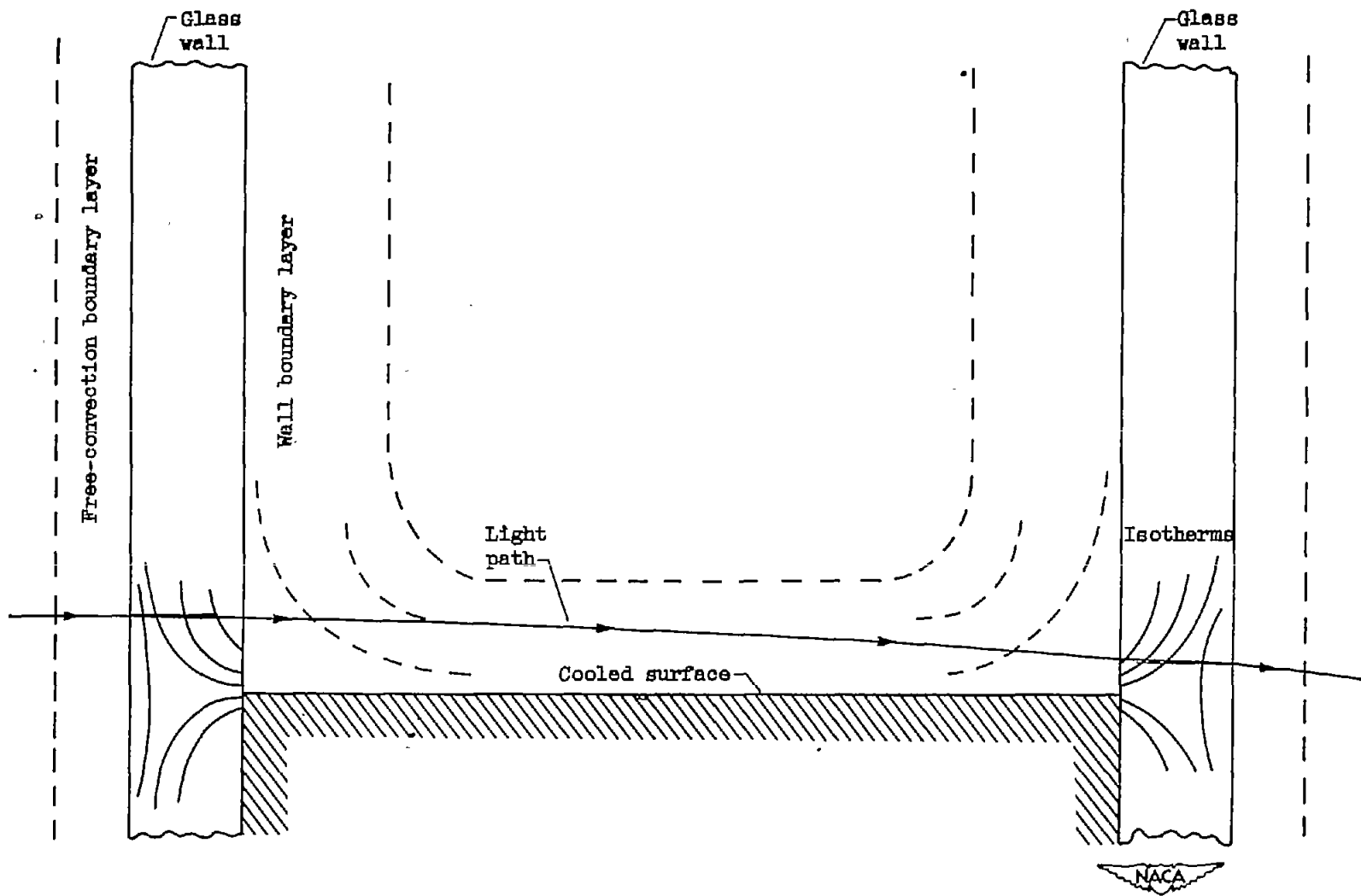
Figure 1. - Schematic diagram of path of light ray through two-dimensional test section.
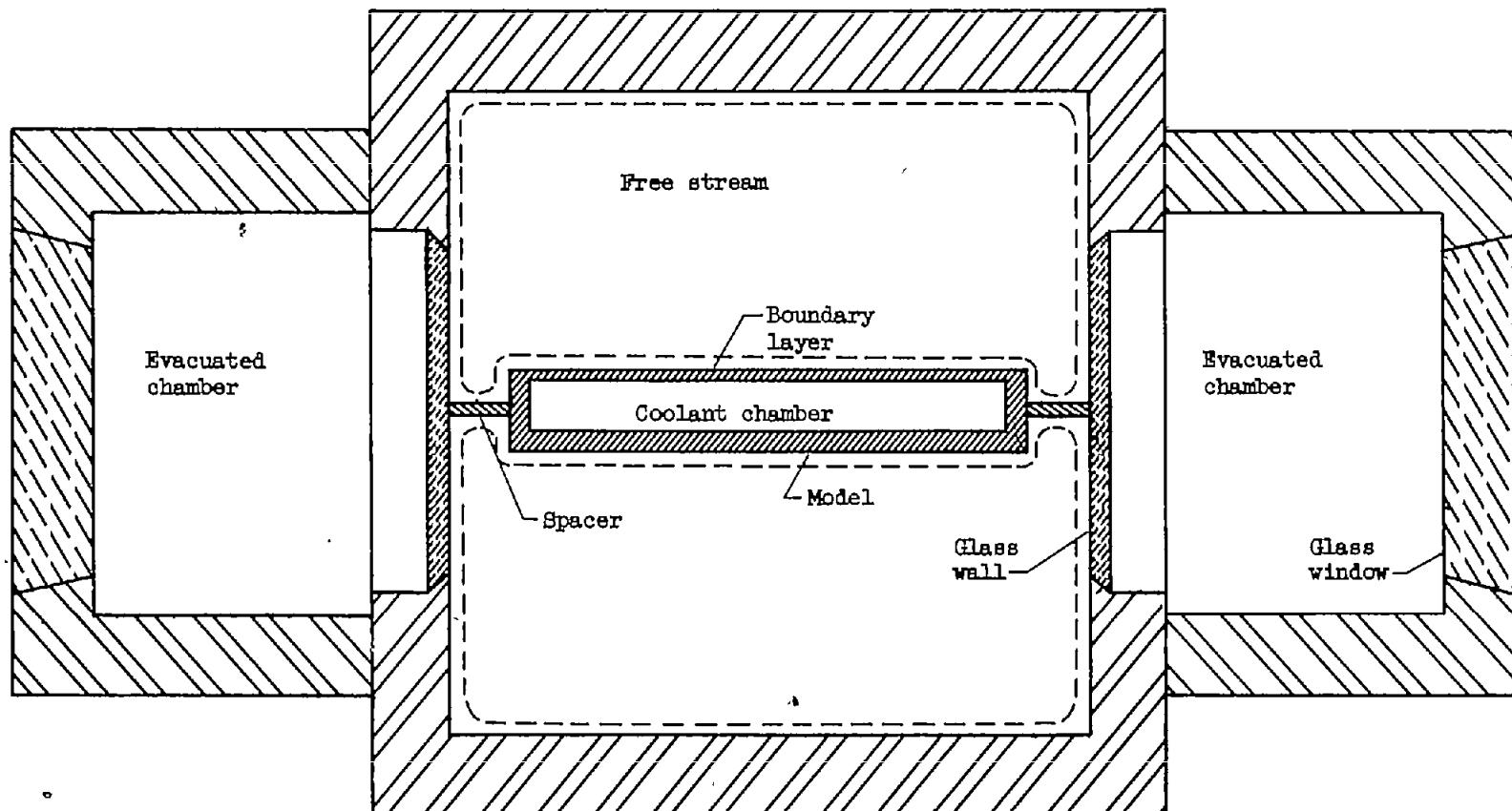
Figure 2. - Cross section of channel for interferometric study of boundary layer on cooled surface.
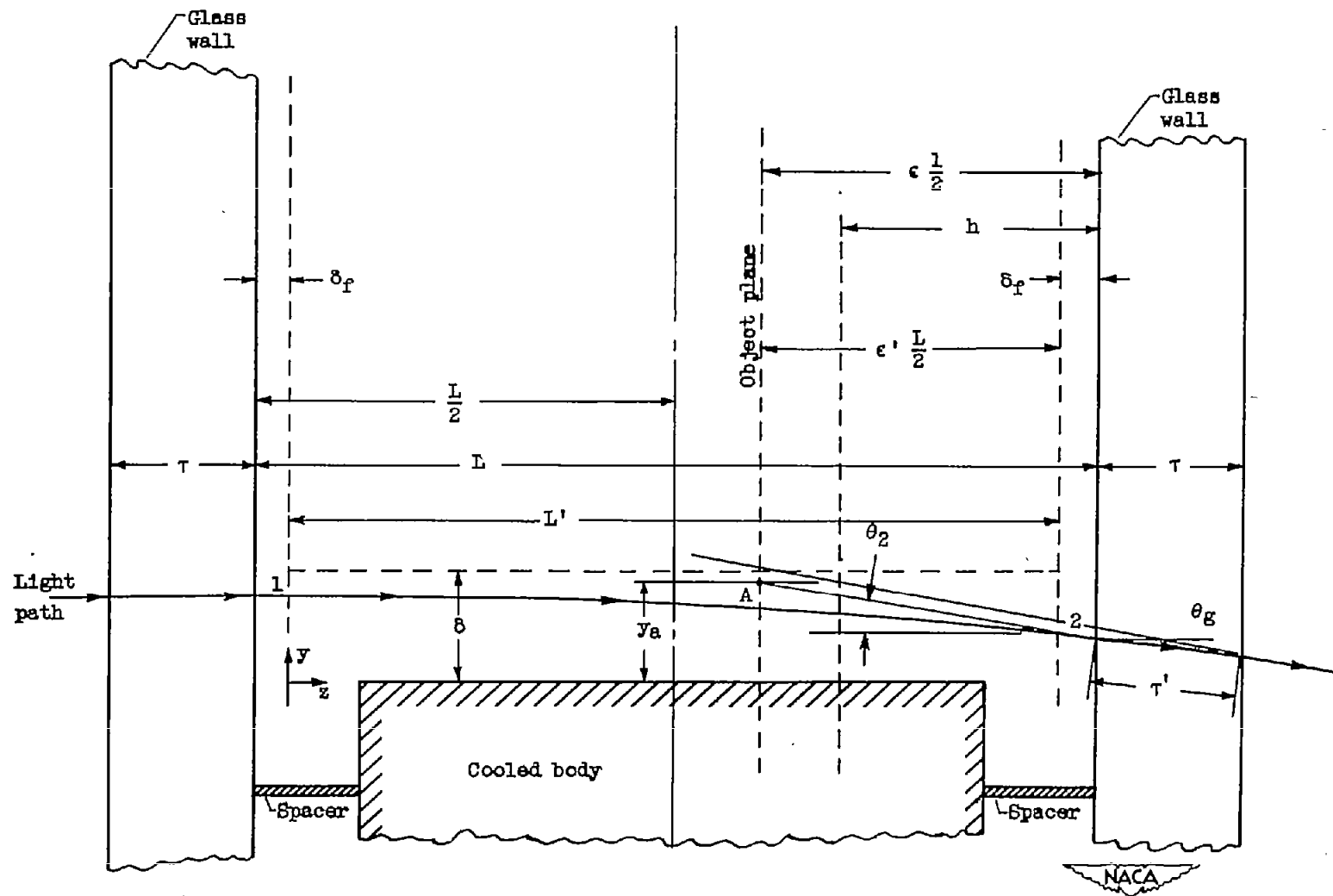
Figure 3. - Path of light ray through boundary layer on cooled body.
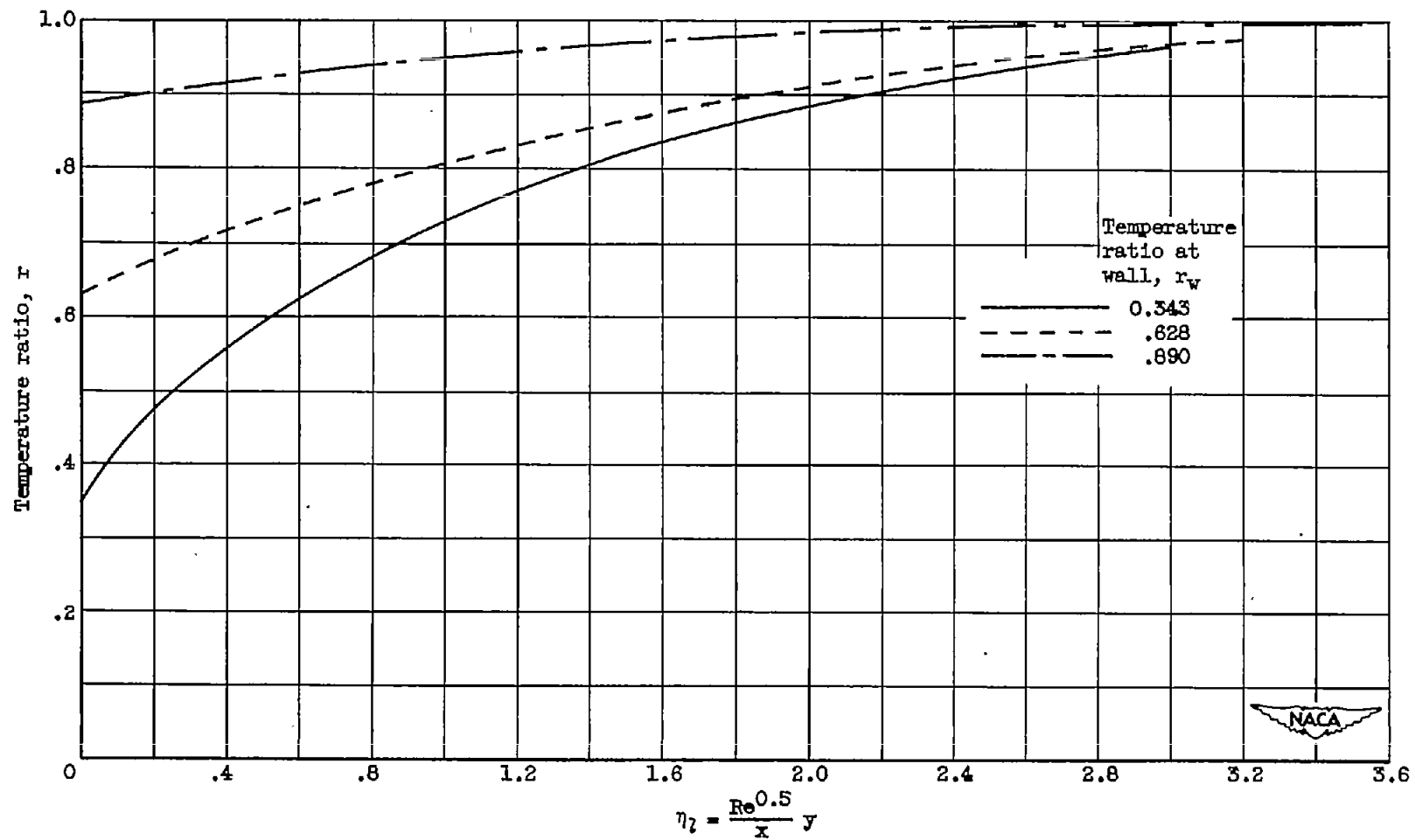
(a) Laminar boundary layer; Pr = 0.725; ω = 0.75; β = 0.19. (Data from reference 4.)

Figure 4. - Temperature profiles; free-stream M_δ = 1.
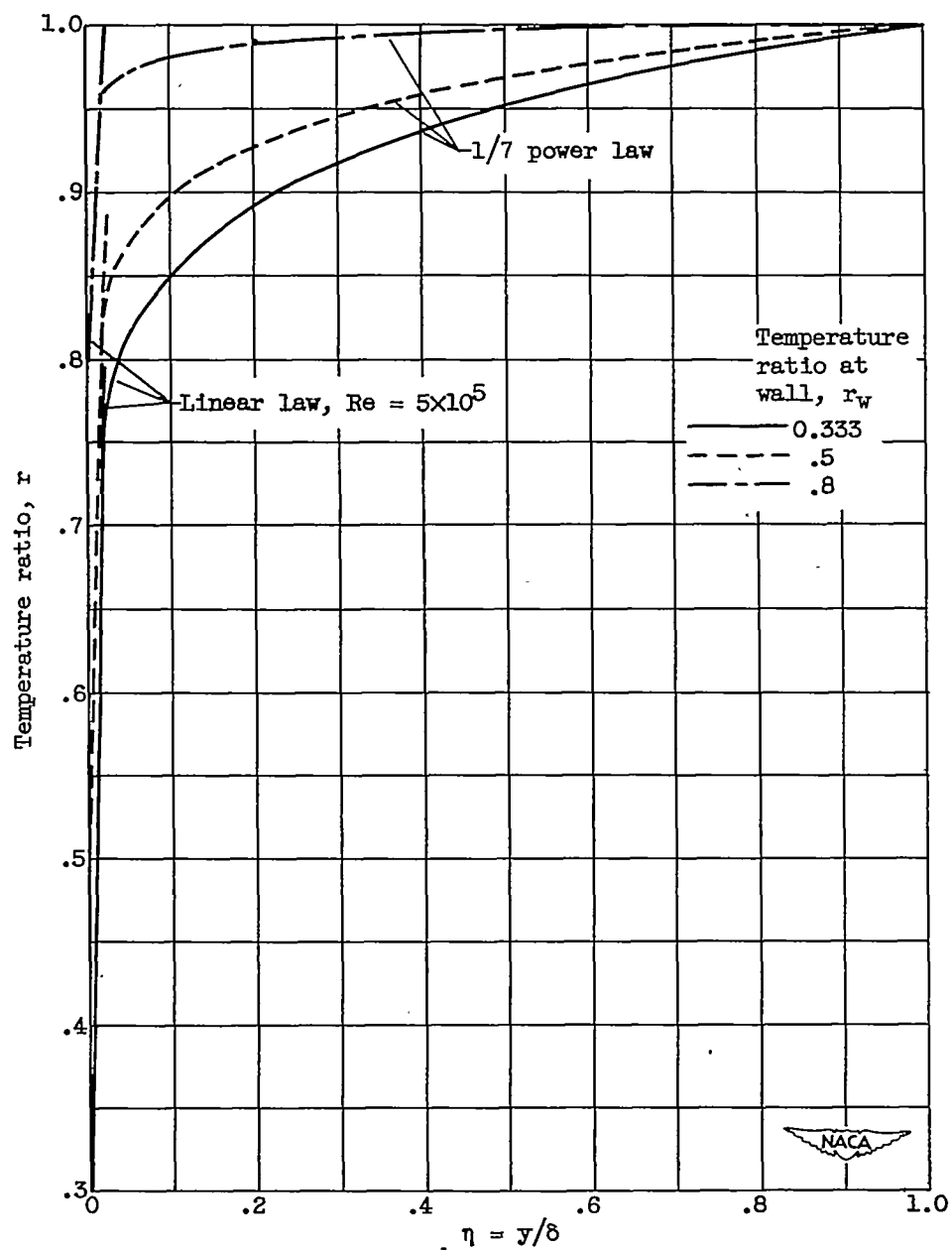
(b) Turbulent boundary layer; $\gamma = 1.4$.

Figure 4. - Concluded. Temperature profiles; free-stream $M_\delta = 1$.

$$\xi_l = 0.5(k\rho_\delta) \ Re(L'/x)^2 \ (x/L')^2$$
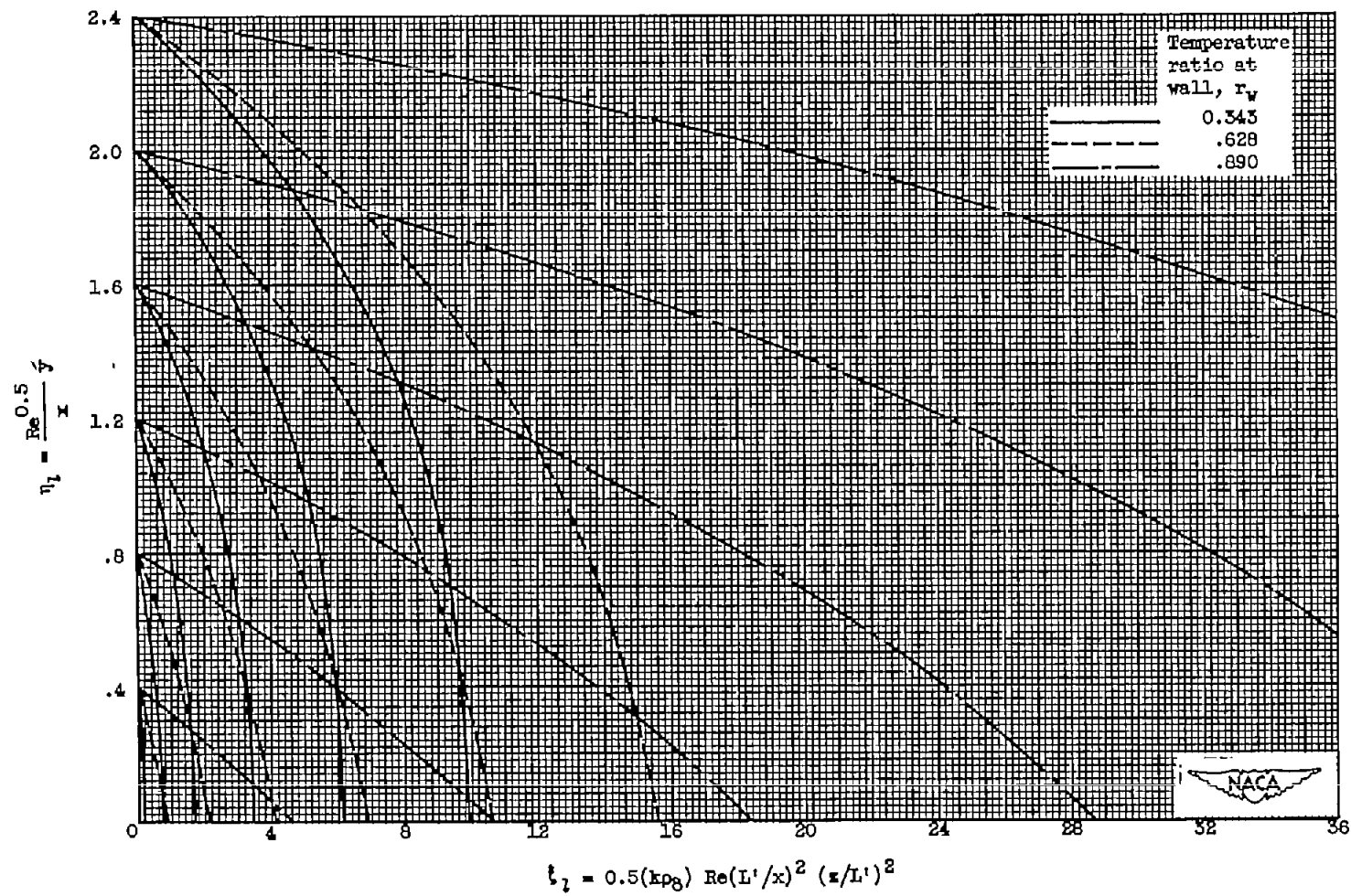
(a) Laminar boundary layer.

Figure 5. - Light-ray paths.
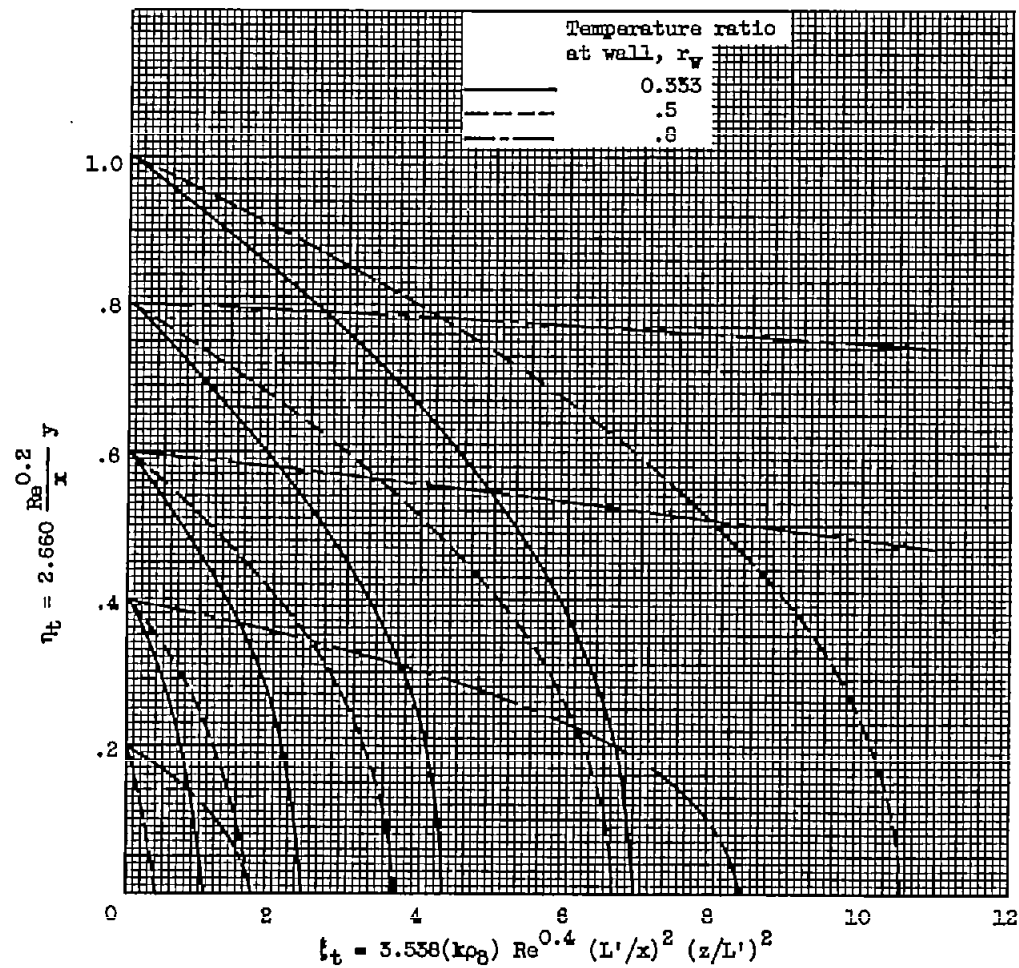
(b) Turbulent boundary layer.

Figure 5. - Concluded. Light-ray paths.
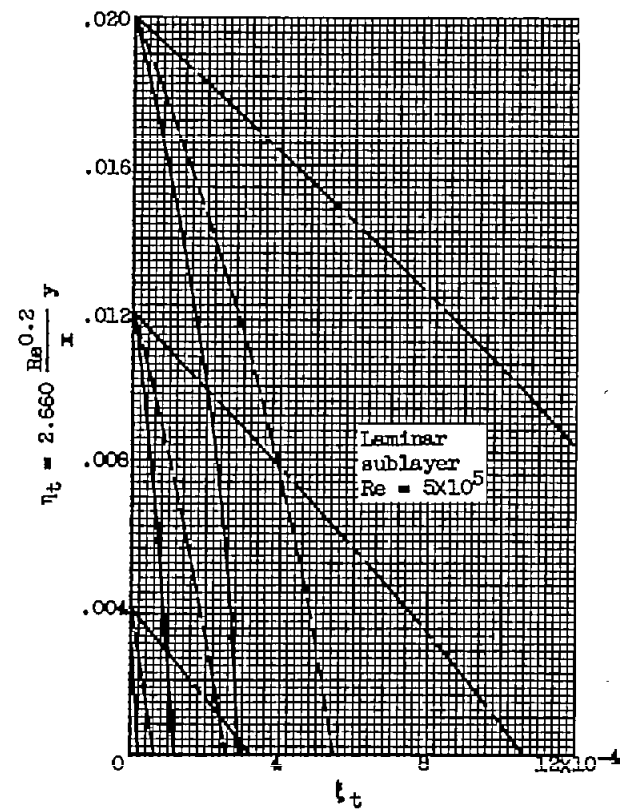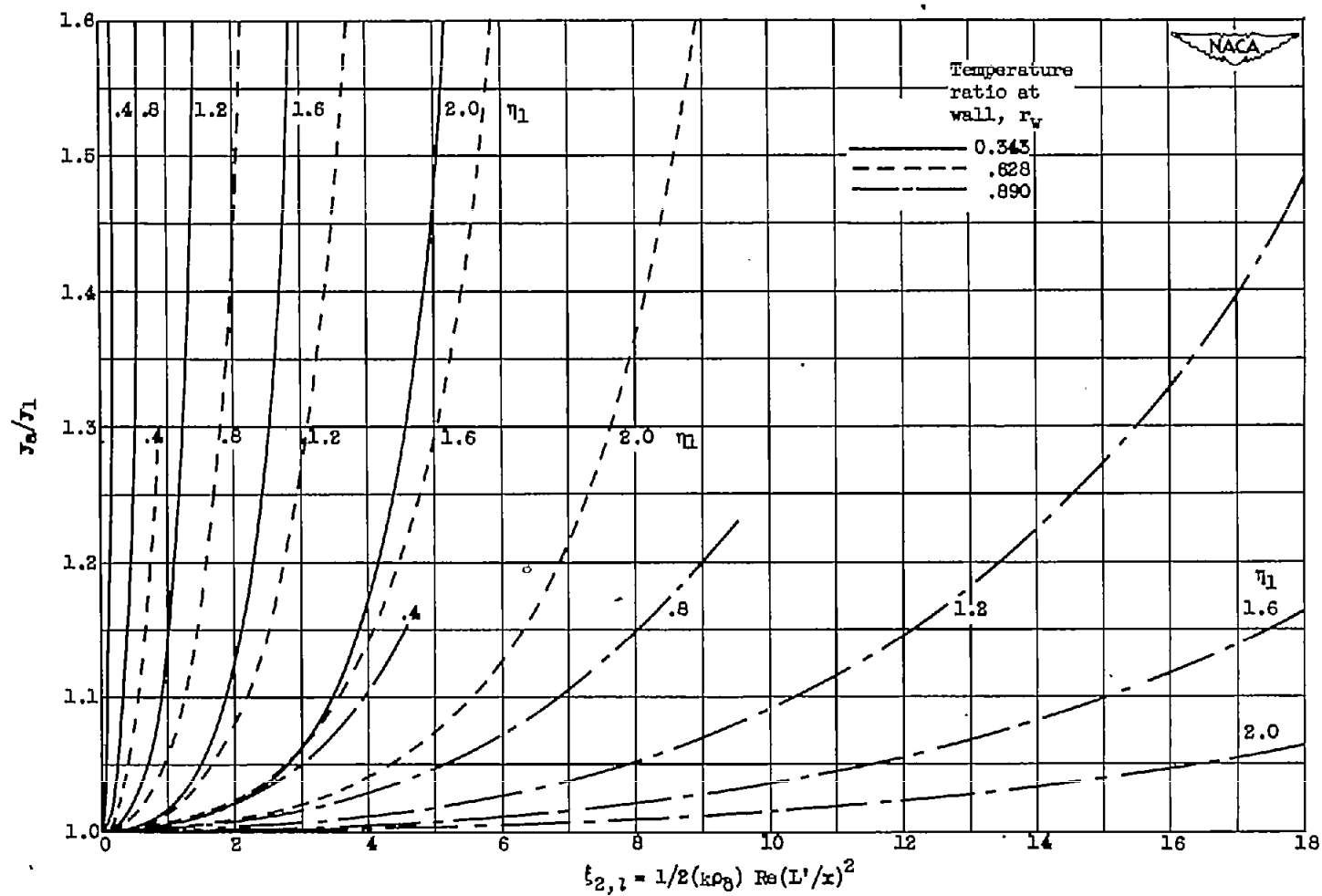
(a) Laminar boundary layer.

Figure 6. – Effect of refraction on position correction; $\epsilon' = 1.0$.
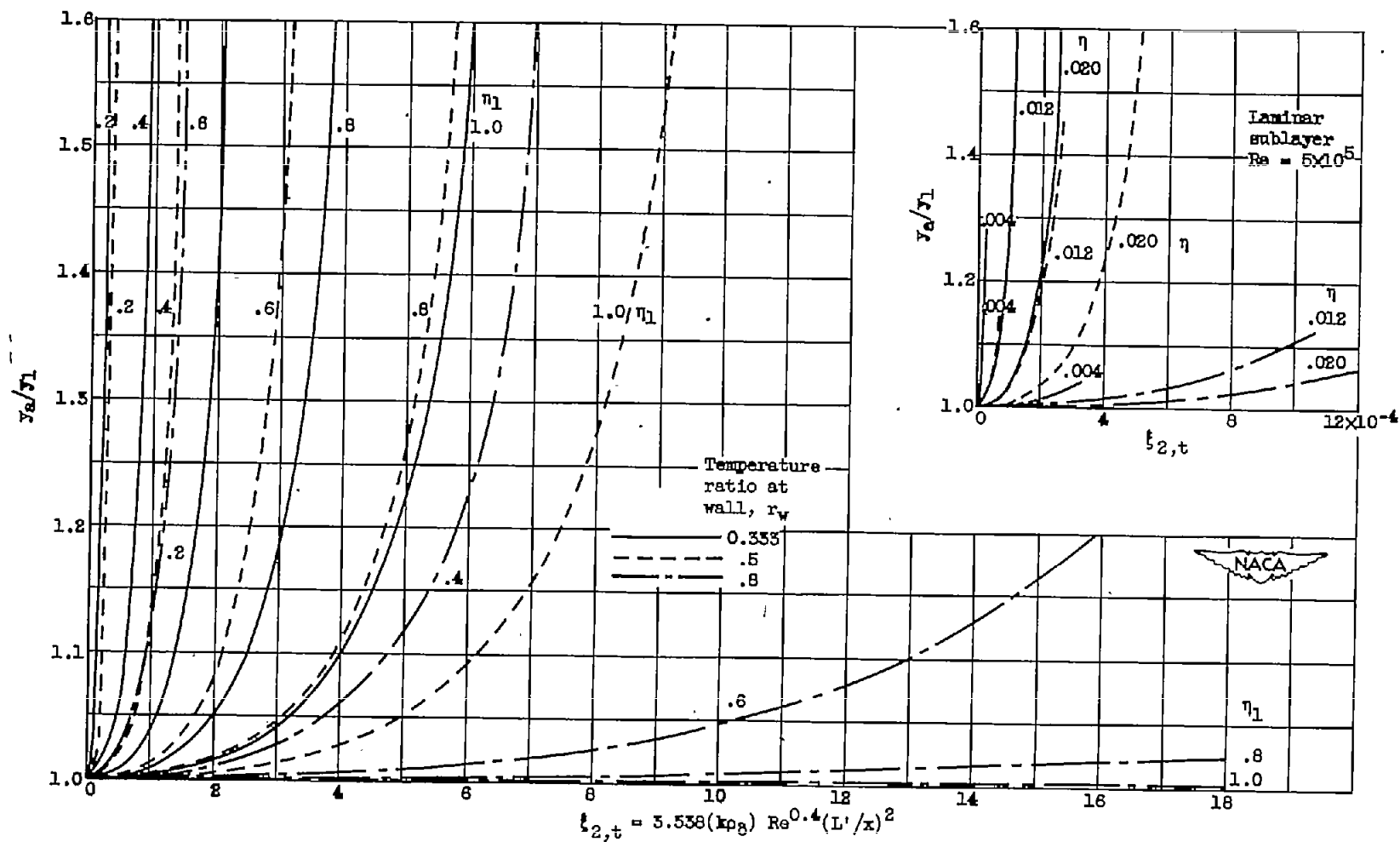
(b) Laminar boundary layer.

Figure 6. - Concluded. Effect of refraction on position correction; $\epsilon' = 1.0$.
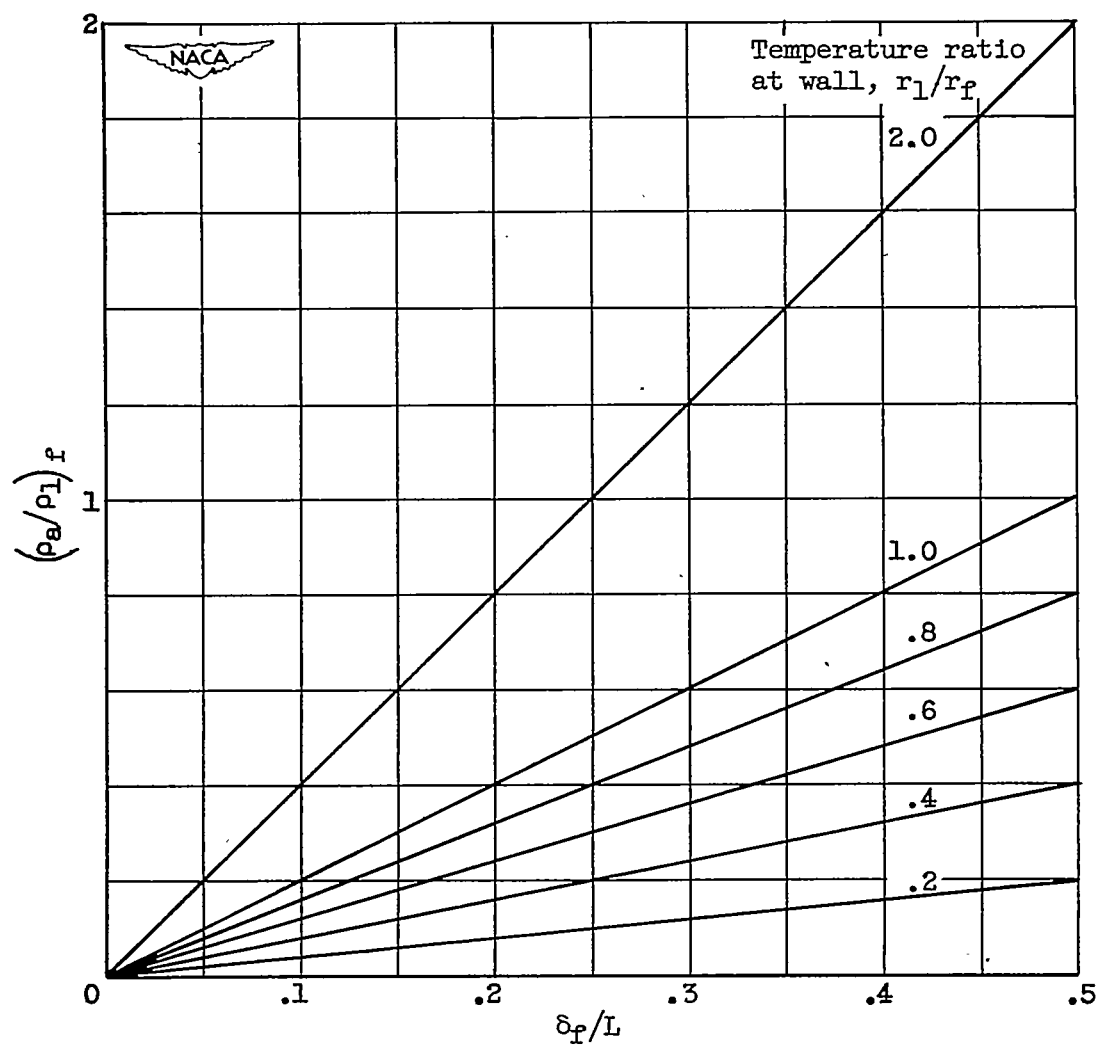
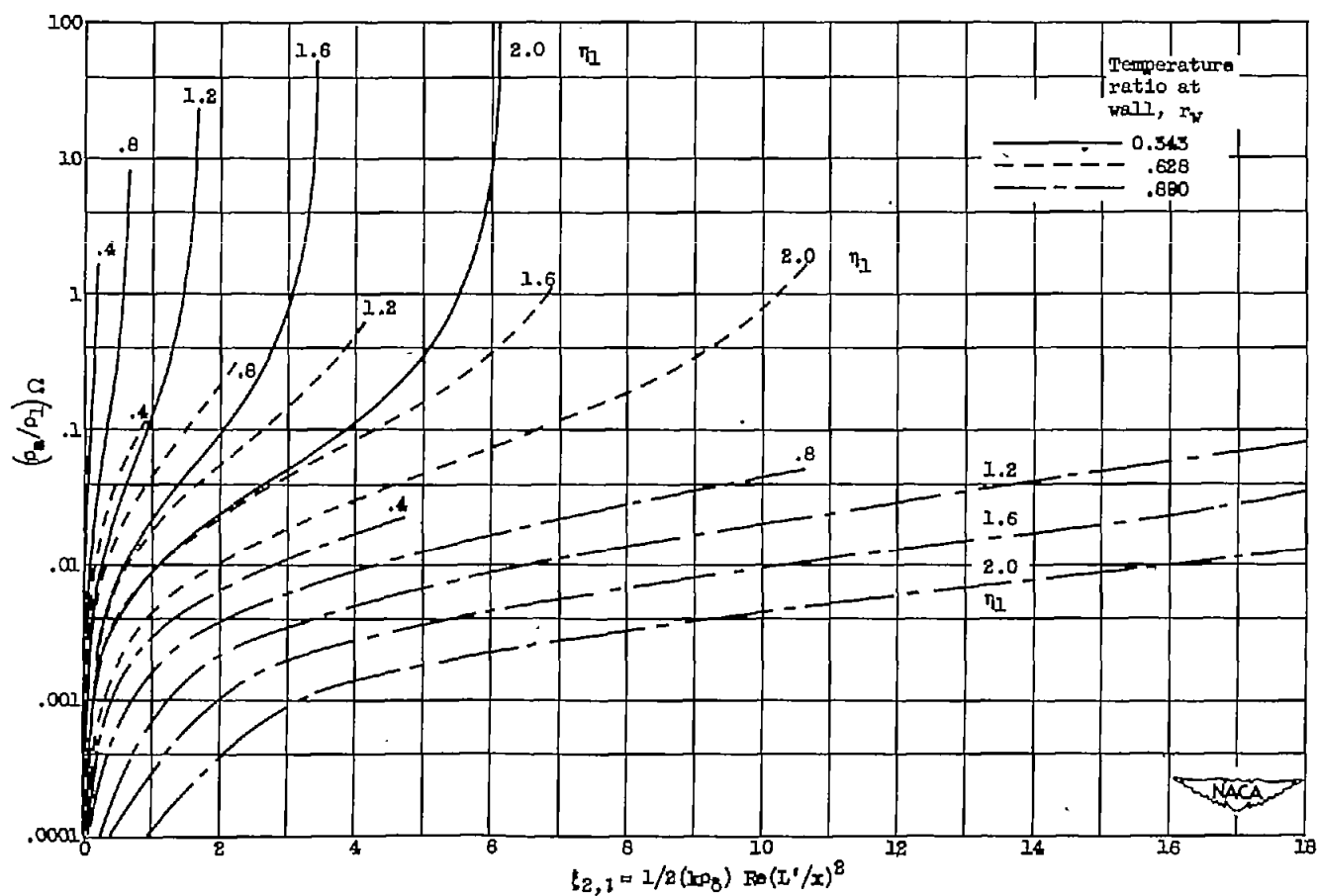Figure 7.- - Effect of wall boundary layer on $\left(\rho_a/\rho_l\right)_f$.
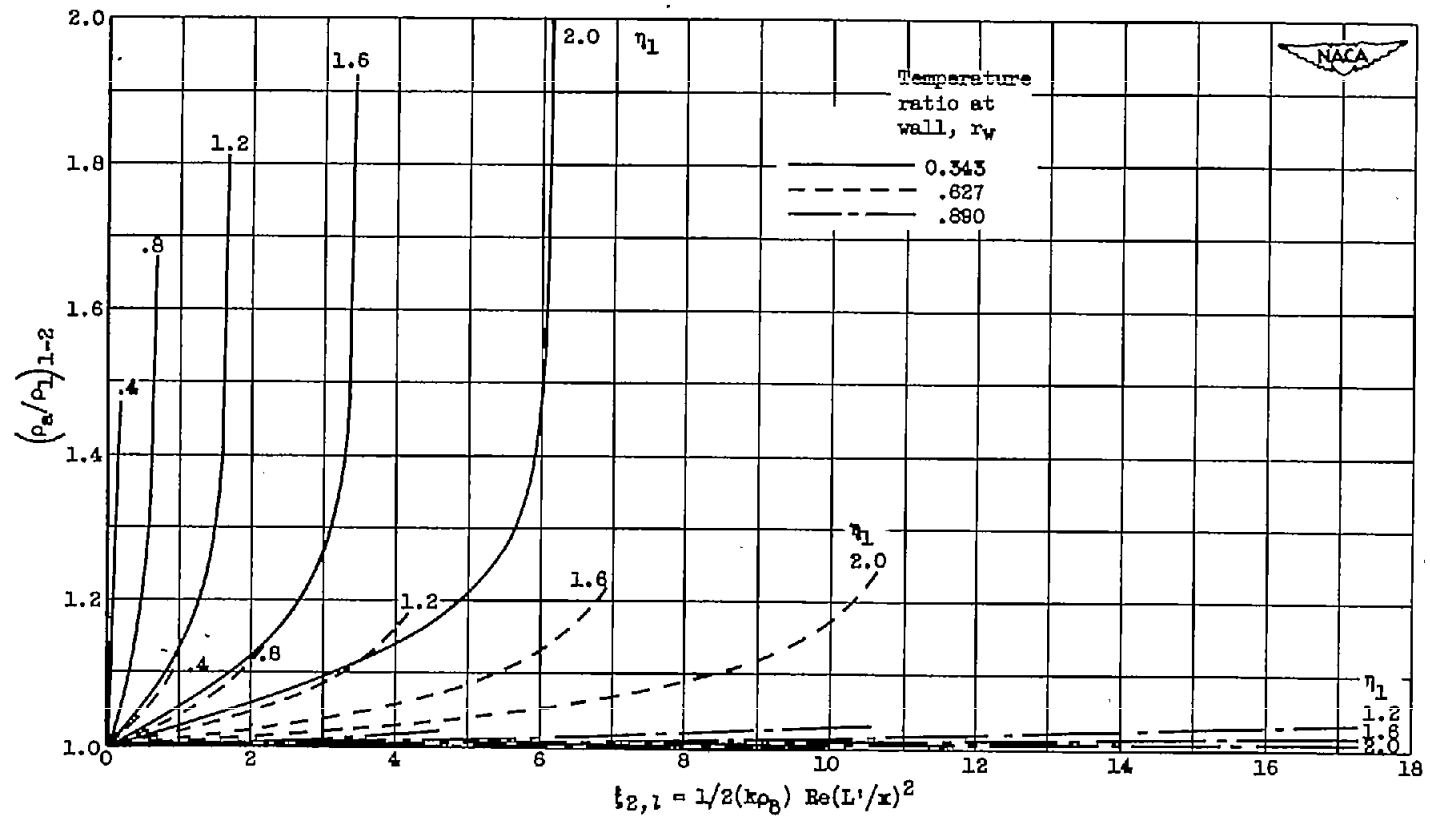
(a) Laminar boundary layer.

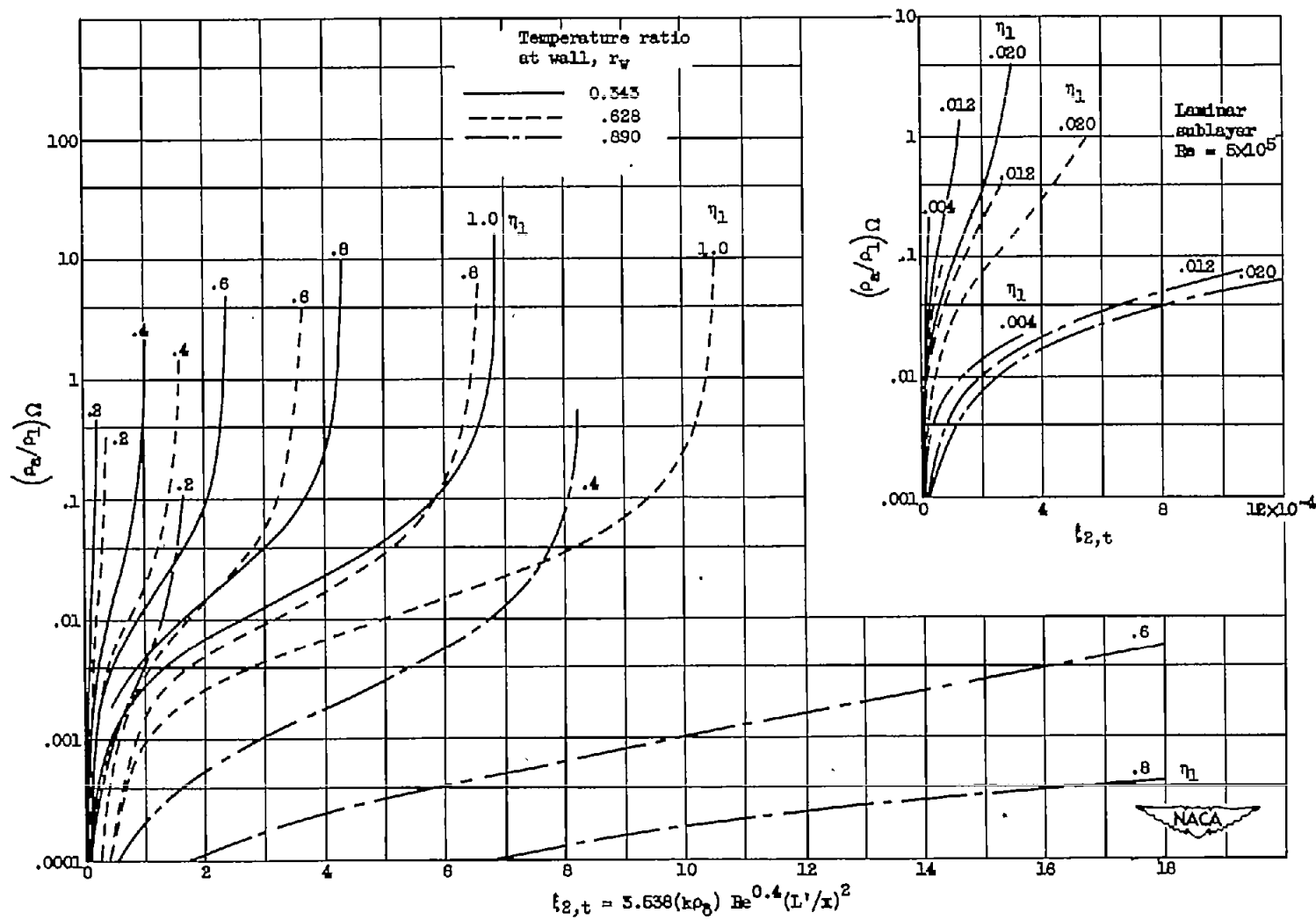Figure 8. - Effect of refraction on $(\rho_a/\rho_1)_{1-2}$; $\delta_f/L = 0$.
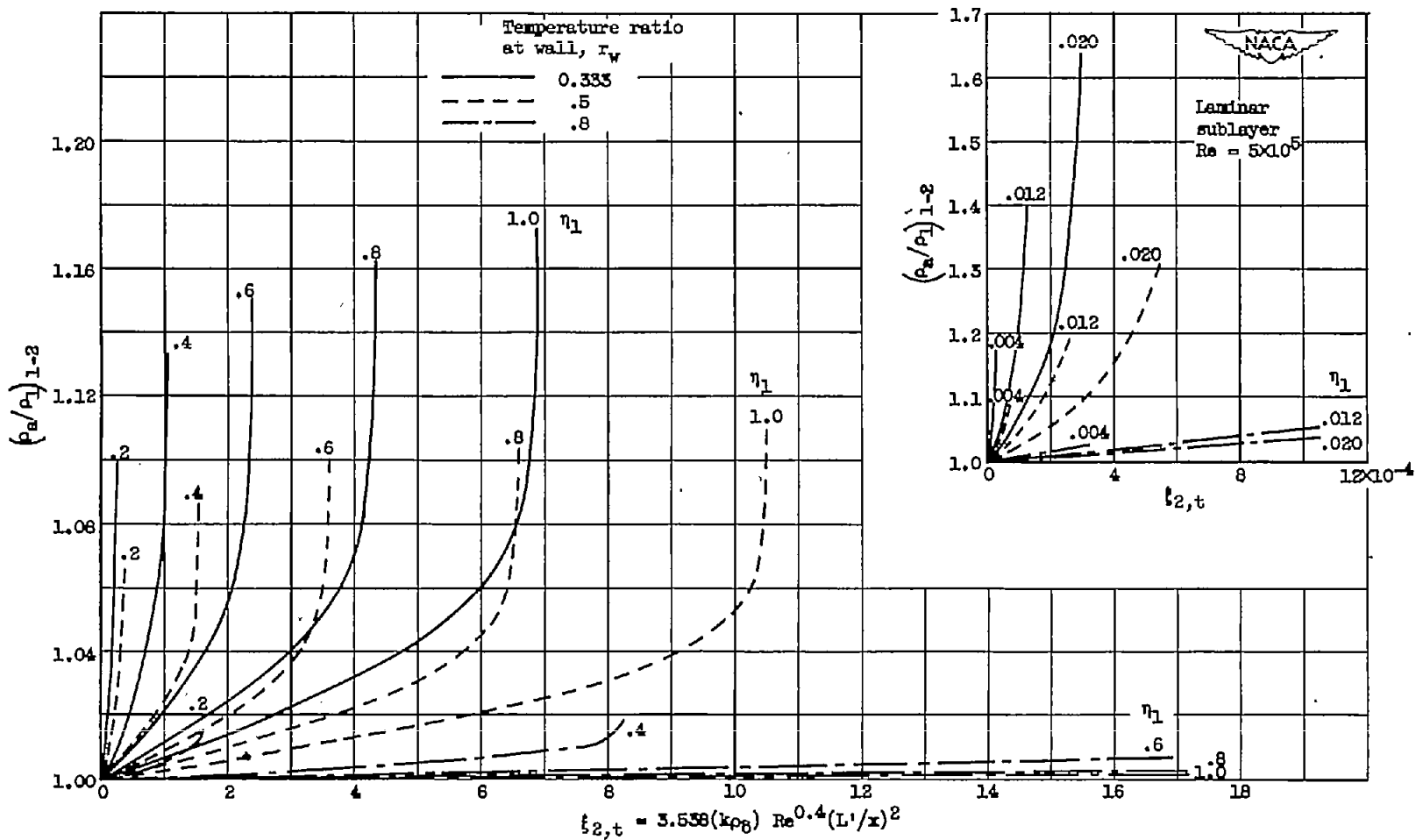
(b) Turbulent boundary layer.

Figure 8. - Concluded. Effect of refraction on $(\rho_a/\rho_1)_{1-2}$; $\delta_f/L = 0$.

(a) Laminar boundary layer.

Figure 9. - Effect of refraction on $(\rho_a/\rho_1)_\Omega$; $\epsilon = 1.0$; $\eta_g = 1.5$.

(b) Turbulent boundary layer.

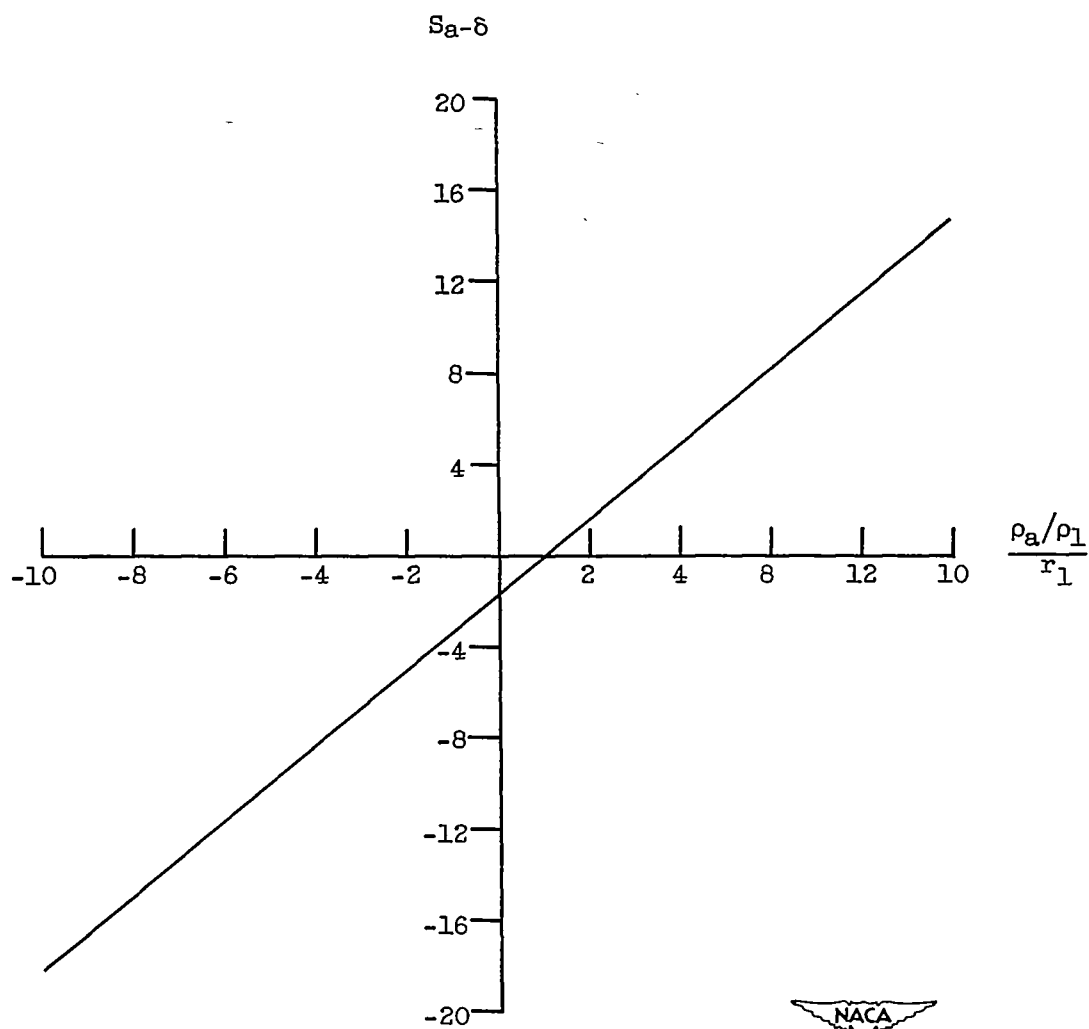Figure 9. – Concluded. Effect of refraction on $(\rho_a/\rho_1)_\Omega$; $\epsilon = 1.0$; $\eta_g = 1.5$.

Figure 10. - Effect of $\dfrac{\rho_a/\rho_1}{r_1}$ on boundary-layer fringe shift; L = 1 inch;

λ = 5461 A; ρ_δ = 0.0000349.